International Journal of Quantum Information
Vol. 8, No. 3 (2010) 505–515

DOI: 10.1142/S0219749910006447

World Scientific
www.worldscientific.com

SOME FEATURES OF THE STATE-SPACE TRAJECTORIES FOLLOWED BY ROBUST ENTANGLED FOUR-QUBIT STATES DURING DECOHERENCE

A. P. MAJTEY

Departament de Fisica, Universitat de les Illes Balears,
Palma de Mallorca, 07122, Spain
anamajtey@gmail.com

A. BORRAS

Departament de Fisica, Universitat de les Illes Balears,
Palma de Mallorca, 07122, Spain

Kavli Institute of Nanoscience, Delft University of Technology,
Lorentzweg 1, 2628 CJ Delft, The Netherlands

A. R. PLASTINO

Instituto Carlos I de Física Teórica y Computacional,
Universidad de Granada, Granada, 18071, Spain

National University La Plata, CREG-Conicet, C.C. 727,
La Plata, 1900, Argentina

M. CASAS

Departament de Fisica and IFISC-CSIC, Universitat de les Illes Balears,
Palma de Mallorca, 07122, Spain

A. PLASTINO

National University La Plata, CCT-Conicet, C.C. 727,
La Plata, 1900, Argentina

Received 14 January 2010

In a recent work (Borras *et al.*, *Phys. Rev. A* **79** (2009) 022108), we have determined, for various decoherence channels, four-qubit initial states exhibiting the most robust possible entanglement. Here, we explore some geometrical features of the trajectories in state space generated by the decoherence process, connecting the initially robust pure state with the completely decohered mixed state obtained at the end of the evolution. We characterize these trajectories by recourse to the distance between the concomitant time-dependent mixed state and different reference states.

Keywords: Entanglement; decoherence.

1. Introduction

Entanglement and decoherence are two closely related phenomena that lie at the core of quantum physics.[1–3] Entanglement is nowadays regarded as the most distinctive feature of quantum mechanics, and in recent years it has been the subject of intense and increasing research efforts. The phenomenon of decoherence consists, basically, of a set of effects arising from the interaction (and concomitant entanglement development) between quantum systems and their environments.[2,3] Every physical system is immersed in an environment and interacts with it in some way. Undesirable effects due to this interaction constitute some of the main obstacles to the practical implementation of quantum technologies based on the controlled manipulation of entangled states such as quantum computing.[2] The decoherence process leads the system from a pure state to a (usually less entangled) mixed state. This decay of entanglement has recently attracted the interest of many researchers.[4–15] It has also been shown that in some cases, entanglement can vanish in finite times. This phenomenon is known as *entanglement sudden death* and it has been the focus of numerous contributions.[16–21] This abrupt disappearance of entanglement is closely related to the *sudden birth of entanglement* between the reservoirs.[22]

Recently, several dynamical properties of entanglement, like asymptotic birth of entanglement and entanglement sudden death, have been discussed from a geometrical point of view.[23,24] These geometrical interpretations allow for the explanation of the necessary and sufficient conditions for the last phenomenon to take place.[23] Various examples according to different possibilities for the geometrical details of the set of time asymptotic states are provided in Ref. 24.

We have recently studied the decay of entanglement under different paradigmatic noisy channels, identifying the initial states exhibiting the most robust entanglement.[4]

The aim of the present contribution is to explore characteristic traits of those state-space trajectories associated to robust states, with emphasis on the study, from a geometrical point of view, of optimal-ones. This will hopefully shed some light on the existence and behavior of robust states. The paper is organized as follows. In Sec. 2, we briefly review the local decoherence models for multi-qubit systems and the entanglement and distance measures that will be used in the present work. In Sec. 3, we investigate the evolution trajectories in state space of highly entangled four-qubit states. Finally, some conclusions are drawn in Sec. 4.

2. Preliminaries

The systems under consideration in the present study consist of an array of N independent qubits initially entangled due to a previous, arbitrary interacting process. Each qubit in the composite system is coupled to its own environment. In such a local-environment formulation there is no communication among qubits and the

entanglement between the subsystems cannot increase because of the locality of the involved operations. We assume that all qubits are affected by an identical decoherence process. The dynamics of any of these qubits is governed by a master equation from which one can obtain a completely positive trace-preserving map ε which describes the corresponding evolution: $\rho_i(t) = \varepsilon\rho_i(0)$. In the Born−Markov approximation these maps (or channels) can be described using its Kraus representation

$$\varepsilon_i \rho_i(0) = \sum_{j=1}^{M} E_{ji} \rho_i(0) E_{ji}^{\dagger}, \tag{1}$$

where E_j $j = 1, \ldots, M$ are the so called Kraus operators, M being the number of operators needed to completely characterize the channel.[25] Using the Kraus operators formalism it is possible to describe the evolution of the entire N-qubit system,

$$\rho(t) = \varepsilon\rho(0) = \sum_{i \cdots j} E_{i1} \otimes \cdots \otimes E_{jN} \rho(0) [E_{i1} \otimes \cdots \otimes E_{jN}]^{\dagger}. \tag{2}$$

2.1. *Decoherence models*

We concentrate our efforts in the study of the following family of decoherence channels: the bit flip (BF), phase flip (PF), and bit-phase flip (BPF). These channels represent all the possible errors in quantum computation, the usual BF $0 \leftrightarrow 1$, the PF, and the combination of both, BPF. The corresponding pair of Kraus operators $\{E_0, E_1\}$ for each channel is given by:

$$E_0 = \sqrt{1 - p/2} I, \quad E_1^i = \sqrt{p/2} \sigma_i; \tag{3}$$

where I is the identity matrix, σ_i are the Pauli matrices, and $i = x$ give us the BF, $i = z$ the PF, and $i = y$ the BPF. Following Salles *et al.*,[11] the factor 2 in Eq. (3) guarantees that at $p = 1$ the ignorance about the occurrence of an error is maximal, and as a consequence, the information about the state is minimum. The results obtained with the phase damping channel are the same as those of the PF channel, actually they can be shown to represent the same process, under a proper change of variables.[2]

We also consider the depolarizing channel (D) which can be viewed as a process in which the initial state is mixed with a source of white noise with probability p. For a d-dimensional quantum system, it can be expressed as

$$\varepsilon\rho = \frac{p}{d} I + (1 - p)\rho. \tag{4}$$

The Kraus operators for this process, including all Pauli matrices are

$$E_0 = \sqrt{1 - p'} I; \quad E_i = \sqrt{\frac{p'}{3}} \sigma_i, \tag{5}$$

where $p' = 3p/2$. Under this process, the state turns separable after a finite time, because this channel is the only one considered in this work exhibiting the phenomenon of entanglement sudden death. We remember here that due to the high symmetry of the depolarizing channel, the evolution of the entanglement depends only on the amount of entanglement of the initial state. Then, according to this process, we obtain equivalent evolutions of the entanglement for initial states which are equivalent under local unitary operation.[4] Some results for this channel will be commented on at the end of Sec. 3.

The parameter p in the channels (3) and (4) is a natural parameterization of time, larger values of p corresponding to later times. In particular, $p = 0$ corresponds to the initial time, when the map ϵ given in Eqs. (1) and (2) coincides with the identity map and no decoherence has taken place. On the other hand, $p = 1$ refers to the asymptotic limit $t \to \infty$.

2.2. *Multipartite entanglement quantification*

One of the most popular measures proposed to quantify multipartite entanglement is based on the use of a bipartite measure, which is averaged over all possible bipartitions of the system. It is mathematically expressed in the fashion

$$E = \frac{1}{[N/2]} \sum_{m=1}^{[N/2]} E^{(m)}, \tag{6}$$

$$E^{(m)} = \frac{1}{N^m_{\text{bipart}}} \sum_{i=1}^{N^m_{\text{bipart}}} E(i). \tag{7}$$

Here, $E(i)$ stands for the entanglement associated with one single bipartition of the N-qubit system. The quantity $E^{(m)}$ gives the average entanglement between subsets of m qubits and the remaining $N - m$ qubits that constitute the system. The average is performed over the ensuing $N^{(m)}_{\text{bipart}}$ nonequivalent bipartitions. If one uses the linear entropy S_L of the reduced density matrix of the smaller bipartition to compute $E(i)$, $E^{(1)}_L$ turns out to be the well-known Meyer−Wallach multipartite entanglement measure.[26] This measure was later generalized by Scott to the case where all possible bipartitions of the system were considered.[27] The Meyer−Wallach multipartite entanglement measure has recently been related to the regularized quantum Fisher information measure which gives the estimation of the strength of low-noise locally depolarizing channels.[28]

We will use the negativity as our bipartite measure of entanglement because we are dealing with mixed states. The negativity is proportional to the sum of the negative eigenvalues α_i of the partial transpose matrix associated with a given bipartition. The properly normalized negativity reads

$$\text{Neg} = \frac{2}{2^m - 1} \sum_i |\alpha_i|. \tag{8}$$

2.3. *Distance measures*

Distance measures between quantum states constitute important tools in quantum information theory.[29−33] In the present work, in order to characterize the trajectories of decohered states, we compute the distances between the state of interest and several reference states, such as the initial, final, and maximally mixed ones. We measure the distance between two different quantum mixed states by recourse to the quantum Jensen Shannon divergence (QJSD), which can be defined in terms of the relative entropy as[29]

$$d_{\mathrm{JS}}(\rho,\sigma)=\frac{1}{2}\left[S\left(\rho,\frac{\rho+\sigma}{2}\right)+S\left(\sigma,\frac{\rho+\sigma}{2}\right)\right], \tag{9}$$

that can be recast in terms of the von Neumann entropy $H_N(\rho)=-Tr(\rho\log\rho)$ in the fashion

$$d_{\mathrm{JS}}(\rho,\sigma)=H_N\left(\frac{\rho+\sigma}{2}\right)-\frac{1}{2}H_N(\rho)-\frac{1}{2}H_N(\sigma). \tag{10}$$

The metric character of the square root of the QJSD has been ascertained recently for pure states, and strong numerical evidences have also been found for the mixed states case.[30,31] To avoid an exclusive dependence on the above distance measure, we also use the Hilbert−Schmidt distance.[32]

$$d_{\mathrm{HS}}(\rho,\sigma)=\|\rho-\sigma\|^2_{\mathrm{HS}}=Tr[(\rho-\sigma)^2]. \tag{11}$$

We will be able to appreciate the fact that the results obtained with both distance measures are qualitatively the same.

2.4. *Robust maximally entangled four-qubit states*

In a previous work, we have performed an iterative numerical search based on the simulating annealing algorithm and determined the initial states that evolve (via the just described noisy channels) to mixed states with the larger possible amount of entanglement.[4] The proof by Higuchi and Sudbery that a four-qubit pure state exhibiting the theoretically maximum amount of entanglement (that is, having all its marginal density matrices maximally mixed) does not exist constituted a landmark in the study of multiqubit entanglement.[34] In Ref. 34, a promising candidate for achieving the maximally entangled state status was also proposed, namely,

$$\begin{aligned}|\Psi^4_{\mathrm{rob}}\rangle \;=\; |\mathrm{HS}\rangle=\frac{1}{\sqrt{6}}[&|1100\rangle+|0011\rangle\\ &+\omega(|1001\rangle+|0110\rangle)+\omega^2(|1010\rangle+|0101\rangle)],\end{aligned} \tag{12}$$

with $\omega=-1/2+i\sqrt{3}/2$. This conjecture has later received support from several numerical studies[36−38] and the $|\mathrm{HS}\rangle$ state has also been shown to constitute a local maximum of the von Neumann entanglement entropy.[35] In our previous work, the $|\mathrm{HS}\rangle$ was found to be a robust state. The concept of robustness used in this work can

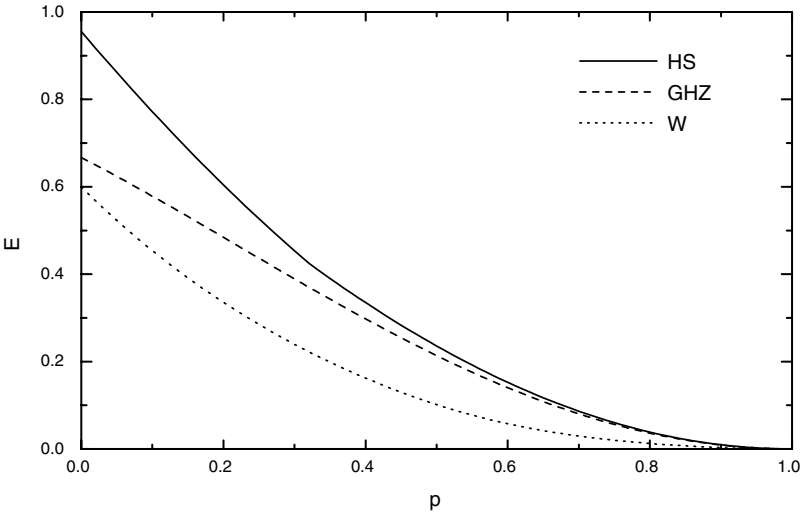

Fig. 1. Entanglement evolution for several four-qubits states under the action of the BF channel. All shown quantities are dimensionless.

be easily explained from Fig. 1. The $|\mathrm{HS}\rangle$ state is considered to be the most robust state because, for any value of p, it leads to decohered states exhibiting more entanglement than those associated with other initial states. In this graph, we plot the entanglement evolution of the $|\mathrm{HS}\rangle$ state under the action of the BF channel and compare it to the entanglement decay of the well-known entangled states $|\mathrm{GHZ}\rangle$ and $|\mathrm{W}\rangle$

$$|\mathrm{GHZ}\rangle = \frac{1}{\sqrt{2}}(|0000\rangle + |1111\rangle), \tag{13}$$

$$|\mathrm{W}\rangle = \frac{1}{2}(|0001\rangle + |0010\rangle + |0100\rangle + |1000\rangle). \tag{14}$$

We also found that, for six-qubit systems the robust state $|\Psi^6_{\mathrm{rob}}\rangle$ turns out to be precisely the maximally entangled state encountered by some of the authors of a previous work.[36] For five-qubit systems, the robust state $|\Psi^5_{\mathrm{rob}}\rangle$ that we found is not as good as the one detected in the four or six qubits instance. For BF and BPF channels, its entanglement becomes lower than that of other states for large p values.[4] The entanglement decays of $|\Psi^4_{\mathrm{rob}}\rangle$ and $|\Psi^6_{\mathrm{rob}}\rangle$ are quite similar and their entanglements are always larger than that of any other state tested in our samplings.

3. Optimal Trajectories

In order to compare the behavior of the entanglement decay for the different channels we compute it in terms of the degree of mixedness, given by the linear entropy of the density matrix of the system (whose evolution is described as a function of the

parameter p)

$$S_L(\rho) = \frac{N}{N-1}(1 - Tr[\rho^2]), \tag{15}$$

where $N = 2^n$ and n is the number of qubits. Here, we display only the results corresponding to four-qubit systems, although similar results are obtained for systems with different number of qubits.

We study the decay of entanglement for different initial states undergoing several decoherence processes. We note that, for those channels for which a given state is robust, the decay of entanglement in terms of the degree of mixedness is the same. In Fig. 2, we plot the decay of entanglement for different four-qubits initial states for BF, PF, and BPF decoherence channels. The entanglement evolution for the $|\mathrm{HS}\rangle$ state coincides for the three considered channels. Remember that the $|\mathrm{HS}\rangle$ state was found to be robust under the action of the three channels studied in this work. In contraposition, the entanglement evolution of the $|\mathrm{GHZ}\rangle$ and $|\mathrm{W}\rangle$ states under the PF channel is not equivalent to that under BF and BPF processes because these states are not robust for the former development.

We also compute the distances between the states (at any given time) and some reference states using the QJSD. We considered as reference states the initial, final, and the maximally mixed state (MM). In Fig. 3, we plot the resultant distances between (i) the mixed state obtained at each time step of the evolution of the initial robust pure state of four-qubits and (ii) the reference states for the previously mentioned decoherence processes. Similar coincident curves (not shown) are obtained for $|\mathrm{GHZ}\rangle$ and $|\mathrm{W}\rangle$ states if we consider only the BF and BPF channels. According to both graphs, the state with robust entanglement (w.r.t. several decoherence

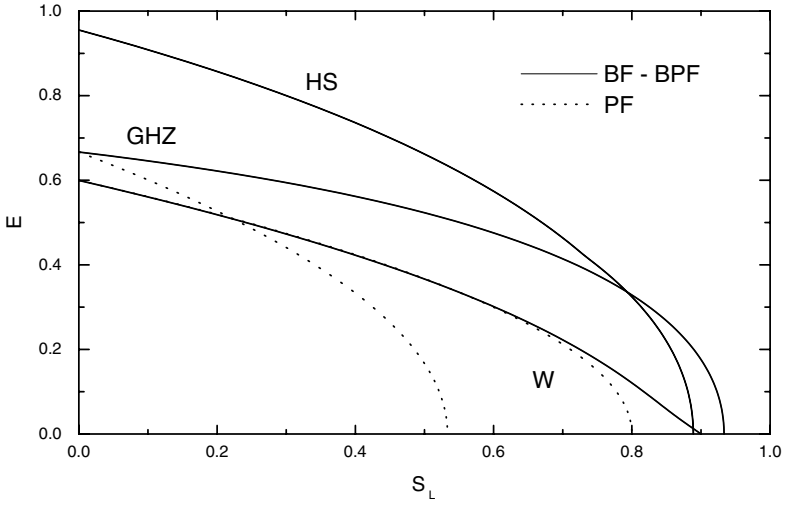

Fig. 2. Entanglement evolution as a function of the linear entropy of four-qubits representative states under phase flip, bit flip, and bit-phase flip decoherence models. All depicted quantities are dimensionless.

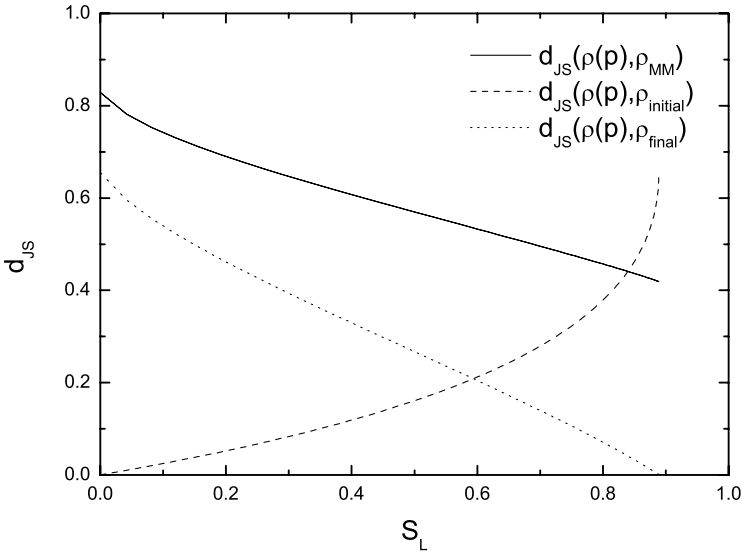

Fig. 3. QJSD between the decohered state (initially $|\Psi^4_{\rm rob}\rangle$) and reference states: maximally mixed state (solid line), initial robust state (dashed line), and final separable state (dotted line). All plotted quantities are dimensionless.

channels) apparently evolves in the same manner under the action of such channels. It is important to note that these trajectories are not actually the same, they are just equivalent.

Finally, we compute the distances between the three final states. These resulting states generated by the PF, BF, and BPF channels when acting upon the initial state $|\Phi_{\rm rob}\rangle$ turn out to be equidistantly distributed, i.e. the distance between any pair of them is always the same. The distance from any of them to the maximally mixed state or to the initial state is also always the same. The overall picture is displayed in Fig. 4. The initial state is represented by the black square, and the three final states are represented by the black spots. These final states are placed at the border of the set of separable states, represented by the grey sphere. The star placed in the middle

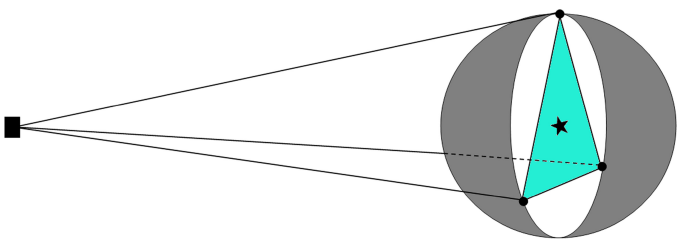

Fig. 4. Equivalent trajectories in Hilbert space, the initial robust four-qubits state is represented by a black square and the final states corresponding to different decoherence processes are represented by black spots at the border of the set of separable states (grey sphere). The star in the center of the sphere represents the MM state.

of the sphere denotes the maximally mixed state. The three decohered trajectories are different but equivalent, and a nice symmetrical configuration is observed.

These results can be extended to robust states in higher dimensions and also to the GHZ and W states under the action of the BF and BPF channels. The results obtained by using the Hilbert−Schmidt distance instead of the QJSD are equivalent. The most representative distances that define the geometry shown in Fig. 3 are given in the following table:

States	d_{JS}	d_{HS}
Initial-final	0.6548	0.9129
Initial-MM	0.8285	0.9682
Final-MM	0.4188	0.3227
Final-final	0.6352	0.4546

As already mentioned, due to its highly symmetric character, the depolarizing channel does not have a single robust state. Any maximally entangled state will be robust for this decoherence process. All the associated trajectories in state space leading to these maximally entangled states are equivalent, and the sudden death of the entanglement always occurs for states with the same degree of mixedness. Systems undergoing this process evolve to a single asymptotic state, i.e. all initial states evolve asymptotically to the MM state. Moreover, they do it following equivalent trajectories. Figure 5 depicts the decay of the entanglement and the linear entropy of

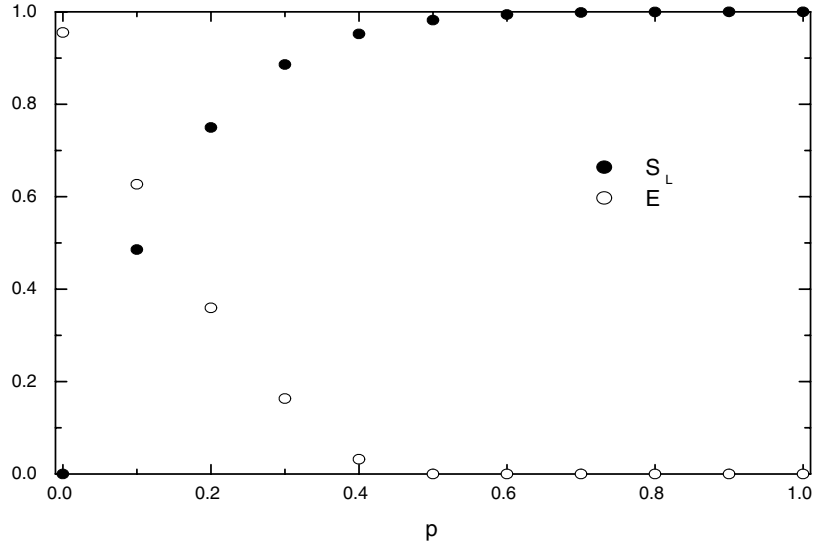

Fig. 5. Entanglement evolution (empty dots) and linear entropy of the time evolved state (filled dots) for 10^3 maximally entangled states obtained from $|\mathrm{HS}\rangle$ by applying local unitary transformations, under depolarizing channel. All plotted quantities are dimensionless.

the decohered state for 10^3 initial maximally entangled states (equivalent under unitary operations) due to the action of the depolarizing channel.

4. Conclusion

In the present work, we have investigated the state-space trajectories associated to previously determined four-qubit robust states undergoing different decoherence processes. We have characterized these trajectories by computing the distance between the time-dependent state resultant from the decoherence process and some fixed states, namely the initial, final, and maximally mixed (MM) states. We have shown that, for states that are robust under decoherence, i.e. those with the maximal amount of entanglement during the evolution, the trajectories' aspect may look different. However, by reference to Fig. 4, one detects a significant degree of equivalence and symmetry among them.

In the case of depolarizing decoherence processes, the final state is the MM-one, but the system becomes separable before reaching it, i.e. a sudden death of entanglement takes place for this process. According to the symmetry of this channel, all maximally entangled states are robust, and they evolve in equivalent fashion. Because of this equivalence, the entanglement's sudden death for any initial maximally entangled state is always characterized by the same degree of mixedness.

Acknowledgments

This work was partially supported by the MEC grant FIS2008-00781 (Spain), by the Project FQM-2445 of the Junta de Andalucia (Spain), by FEDER (EU), and by Conicet (Argentine Agency). AB acknowledges support from MEC through FPU fellowship AP-2004-2962 and APM acknowledges support of MEC contract SB-2006-0165.

References

1. I. Bengtsson and K. Zyczkowski, *Geometry of Quantum States: An Introduction to Quantum Entanglement* (Cambridge University Press, Cambridge, 2006).
2. M. A. Nielsen and I. L. Chuang, *Quantum Computation and Quantum Information* (Cambridge University Press, Cambridge, 2000).
3. M. Schlosshauer, *Rev. Mod. Phys.* **76** (2005) 1267.
4. A. Borras *et al.*, *Phys. Rev. A* **79** (2009) 022108.
5. C. Simon and J. Kempe, *Phys. Rev. A* **65** (2002) 052327.
6. A. R. R. Carvalho *et al.*, *Phys. Rev. Lett.* **93** (2004) 230501.
7. W. Dür and H. J. Briegel, *Phys. Rev. Lett.* **92** (2004) 180403.
8. M. Hein *et al.*, *Phys. Rev. A* **71** (2005) 032350.
9. L. Aolita *et al.*, *Phys. Rev. Lett.* **100** (2008) 080501.
10. M. P. Almeida *et al.*, *Science* **316** (2007) 579.
11. A. Salles *et al.*, *Phys. Rev. A* **78** (2008) 022322.
12. L. Aolita *et al.*, *Phys. Rev. A* **79** (2009) 032322.

13. O. Gühne *et al.*, *Phys. Rev. A* **78** (2008) 060301.
14. F. Bodoky *et al.*, *J. Phys. Cond. Mat.* **21** (2009) 395602.
15. S. Campbell *et al.*, *New J. Phys.* **11** (2009) 073039.
16. T. Yu and J. H. Eberly, *Phys. Rev. Lett.* **93** (2004) 140404.
17. T. Yu and J. H. Eberly, *Science* **323** (2009) 598.
18. A. Al-Qasimi and D. F. V. James, *Phys. Rev. A* **77** (2008) 012117.
19. Y. S. Weinstein, *Phys. Rev. A* **79** (2009) 012318.
20. I. Sainz and G. Bjork, *Int. J. Quant. Inf.* **7** (2009) 245.
21. Y.-J. Zhang and Y.-Y. Xia, *Int. J. Quant. Inf.* **7** (2009) 949.
22. C. E. López *et al.*, *Phys. Rev. Lett.* **101** (2008) 080503.
23. M. O. Terra Cunha, *New J. Phys.* **9** (2007) 237.
24. R. C. Drumond and M. O. Terra Cunha, *J. Phys. A: Math. Theor.* **42** (2009) 285308.
25. K. Kraus, *States, Effect, and Operation: Fundamental Notions in Quantum Theroy* (Springer-Verlag, Berlin, 1983).
26. D. A. Meyer and N. R. Wallach, *J. Math. Phys.* **43** (2002) 4273.
27. A. J. Scott, *Phys. Rev. A* **69** (2004) 052330.
28. S. Boixo and A. Monras, *Phys. Rev. Lett.* **100** (2008) 100503.
29. A. P. Majtey *et al.*, *Phys. Rev. A* **72** (2005) 052310.
30. P. W. Lamberti *et al.*, *Phys. Rev. A* **77** (2008) 052311.
31. J. Briët and P. Harremoës, *Phys. Rev. A* **79** (2009) 052311.
32. V. Vedral and M. Plenio, *Phys. Rev. A* **57** (1998) 1619.
33. J. Calsamiglia *et al.*, *Phys. Rev. A* **77** (2008) 032311.
34. A. Higuchi and A. Sudbery, *Phys. Lett. A* **273** (2000) 213.
35. S. Brierley and A. Higuchi, *J. Phys. A: Math. Gen.* **40** (2007) 8455.
36. A. Borras *et al.*, *J. Phys. A: Math. Gen.* **40** (2007) 13407.
37. A. Borras *et al.*, *Int. J. Quant. Inf.* **6** (2008) 605.
38. P. Facchi *et al.*, *Phys. Rev. A* **77** (2008) 060304(R).